Operational Wave, Current, and Wind Measurements With the Pisces HF Radar

Lucy R. Wyatt, J. Jim Green, Andrew Middleditch, Mike D. Moorhead, John Howarth, Martin Holt, and Simon Keogh

Abstract—**This paper presents results of a trial of a Pisces HF radar system aimed at assessing its use as a component of a wave-monitoring network being installed around the coasts of England and Wales. The radar system has been operating since December 2003 and the trial continued to June 2005. The data have been processed in near-real time and displayed on a website. Radar measurements of the directional spectrum and derived parameters are compared with those measured with a directional waverider and with products from the Met Office, United Kingdom, operational wave model. Radar measurements of currents and winds are also compared with Met Office model products and, in the case of winds, with the QuikSCAT scatterometer. Statistics on data availability and accuracy are presented. The results demonstrate that useful availability and accuracy in wave and wind parameters are obtained above a waveheight threshold of 2 m and at ranges up to 120 km at the radar operating frequencies (7–10 MHz) used. Waveheight measurements above about 1 m can be made with reasonable accuracy (e.g., mean difference of 2.5% during January–February 2004). Period and direction parameters in low seas are often contaminated by noise in the radar signal. The comparisons provide some evidence of wave model limitations in offshore wind and swell conditions.**

Index Terms—**Directional waverider buoy, HF radar, model, ocean wave measurement, QuikSCAT, surface current, tide, wind.**

I. INTRODUCTION

THE use of high-frequency (HF) radar systems to measure surface currents has been operational for many years (see, for example, [1]–[8]). Currents are obtained from radar Doppler shift measurements with accuracies that depend on a number of factors including power spectrum frequency resolution, temporal and spatial variability in the measurement cell, and the angle between two radar look directions. These measurements use the first-order backscattered signal which can usually be identified for both phased-array radars (e.g., ocean surface current radar (OSCR) [9] and Pisces [10]) or direction-finding radars [e.g., coastal ocean dynamics application radar (CODAR) [11] and SeaSonde]. The WEllen RAdar (WERA) HF radar system [12] has both phased-array and direction-finding options. To obtain wave measurements, good signal-to-noise (greater than 15 dB) in the second-order part of the backscatter spectrum is needed. This is more difficult to obtain and operational wave measurement has only recently become a possibility. Empirical methods for determining waveheight and period have been developed (see, for example, [13]–[16]). The directional spectrum and derived wave parameters can be obtained using numerical inversion of a nonlinear integral equation [17]–[21], [22]–[29]. Accuracy depends on radar power spectrum frequency resolution, temporal and spatial variability in the measurement cell, angle between two radar look directions, antenna sidelobe levels, and waveheight, noise, and interference levels. Phased-array radars can provide wave measurements with the same spatial and temporal resolution as for current measurements although over more restricted ranges due to the increased signal-to-noise requirement for second-order backscatter. Direction-finding radars only provide these measurements at one range and, unless the system is deployed on an open ocean platform, homogeneity over the whole of this range is assumed and a deep-water equivalent spectrum is estimated assuming onshore wave propagation influenced only by depth refraction.

Wind measurement requires a mix of first- and second-order information. Wind direction can be obtained using the first-order peaks and a two-parameter short wave directional model fitting technique [30]. Accuracy depends on the model used, temporal and spatial variability in the measurement cell, angle between two radar look directions, antenna sidelobe levels, and noise and interference levels. Methods to measure wind speed using empirical models have been developed but a robust method has yet to be demonstrated.

The OSCR and Pisces HF radars were developed in the United Kingdom for oceanographic measurement during the 1980s. OSCR was designed for short-range surface current measurement and Pisces for longer range wave measurement which was demonstrated during the Netherlands/U.K. Radar, Wavebuoy Experimental Comparison (NURWEC) experiments [31], [32]. New methods for detailed directional spectrum measurement were developed at Sheffield, U.K., during the 1990s and were tested during two European funded projects Surface Current And Wave Variability EXperiments (SCAWVEX) [33] and EUROpean Radar Ocean SEnsing (EuroROSE) [34], and in the United States during SHOaling Waves EXperiment

Manuscript received November 15, 2004; accepted September 1, 2006. This work was supported in part by the U.K. Department for Environment Food and Rural Affairs (DEFRA) and the U.K. Natural Environment Research Council (NERC) under Grant NER/A/S/2001/00453. **Associate Editor: M. L. Heron**.

L. R. Wyatt and J. J. Green are with the Sheffield Centre for Earth Observation Science, Department of Applied Mathematics, University of Sheffield, Sheffield S3 7RH, U.K. (e-mail: l.wyatt@sheffield.ac.uk; j.j.green@sheffield.ac.uk).

A. Middleditch was with the Sheffield Centre for Earth Observation Science, Department of Applied Mathematics, University of Sheffield, Sheffield S3 7RH, U.K. He is now with Seaview Sensing Ltd., Sheffield S10 3GR, U.K. (e-mail: andrewmiddleditch@seaviewsensing.com).

M. D Moorhead is with Neptune Radar Ltd, Gardiner's Farm, Sandhurst, Gloucester GL2 9NW, U.K. (e-mail: seawaves@enterprise.net).

J. Howarth is with Proudman Oceanographic Laboratory, Joseph Proudman Building, Liverpool L3 5DA, U.K. (e-mail: mjh@pol.ac.uk).

M. Holt and S. Keogh are with U.K. Met Office, Exeter, Devon EX1 3PB, U.K. (e-mail: martin.holt@metoffice.gov.uk; simon.keogh@metoffice.gov.uk).

Color versions of one or more of the figures in this paper are available online at http://ieeexplore.ieee.org.

Digital Object Identifier 10.1109/JOE.2006.888378

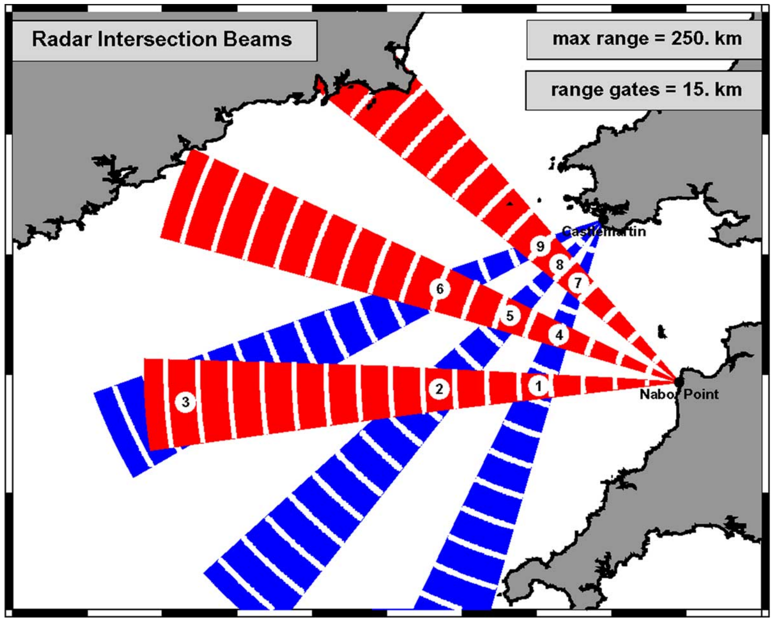

Fig. 1. Radar sites (Nabor Point and Castlemartin), beams, range cells, and nine dual intersection points. The lower left-hand corner of the figure is at 50° N, 9° W, and the graticule increments are every 30′.

(SHOWEX) [35]. The EuroROSE experiments provided the first opportunity to demonstrate real-time wave measurements. Inversion times are around 1/6 s per cell, <1 min for an inversion of $\sim$300 measurement cells.

The U.K. Department for Environment, Food and Rural Affairs (DEFRA), is developing a wave-monitoring network around England and Wales to provide the data needed for a near-shore wave climatology to aid in coastal engineering and design studies and also for improved coastal flood prediction and erosion studies. A number of wave buoys have been deployed and their data can be seen on and downloaded from a dedicated website.

There are locations around the coast where deployment of a buoy is difficult for shipping and fishing reasons or where significant spatial variation in the wave field exists. To deal with these circumstances, DEFRA is trialing the Pisces HF radar system to decide whether such radars can make a useful contribution to the network. After a six month trial with a single system (which can only provide wave parameters, e.g., significant waveheight) a trial of a dual radar system with full measurement capability began in December 2003 and continued until June 2005. This paper presents some results from the first few months of that trial.

II. Pisces HF Radar

Pisces is a frequency modulated interrupted continuous wave (FMICW) radar operating at frequencies in the lower half of the HF band designed to obtain metocean measurements to about 200 km. It was developed by Neptune Radar Ltd., Gloucester, U.K., from a University of Birmingham prototype. The radar operates at frequencies between 5 and 15 MHz with a mean power of up to 1200 W. It uses FMICW modulation enabling monostatic operation without transmitter noise or power limitations and with the ability to focus the peak radar performance at the longest range. It has a 33-m-high log periodic transmit antenna occupying an area of 80×40 m^2 and a receive array of elevated feed monopoles occupying an area 200×10 m^2. Other antenna arrangements are used for some applications.

Bandwidths in the range 8–250 kHz are available, providing range resolutions of 20 to 0.75 km. To maintain a directionally unbiased resolution cell for metocean data requires range and azimuth resolution to be approximately matched, giving a range resolution of 7.5–20 km for long ranges and 2–6 km for short ranges. Programmable settings allowing easy changes to a wide range of radar parameters such as coherent integration time, observation duration, resolution, and power or signal processing. This allows different types of observation to be interleaved, every 5 min or less if required for different applications, through an efficient tasking system providing fully automatic operation.

Trials of a single Pisces radar to demonstrate range and availability for Met Office applications began in 2001. Trials with a dual system, capable of full directional wave spectrum and vector current measurements, were completed in June 2005. One radar is located at Nabor Point, North Devon and the second at Castlemartin, South Wales (see Fig. 1). Both have three fixed-beam positions with low sidelobes which were used sequentially dwelling for about 19 min on each thus giving hourly coverage across the region. A range resolution of 15 km was used for the trial. The radar was operating at a number of frequencies in the 5–11-MHz band varying from hour to hour to minimize as far as possible the impact of interference. For this trial, the radar was configured to provide a maximum range of about 150 km. As a result, the far range intersection point (number 3 in Fig. 1) which is more than 200 km from each radar did not produce usable data. Radar data [Doppler (power) spectra and single radar metocean data] were transmitted via file transfer protocol (ftp) to a metocean data server at Sheffield for further processing. The data presented here were processed by the University of Sheffield, U.K. After the first six months of the trial, this aspect of the work was carried out by Seaview Sensing Ltd, Sheffield, U.K. Wave directional spectra and other metocean measurements were displayed on a website at Sheffield within 10 min of the end of the radar data collection period.

Radar data in the form of Doppler spectra were available for 93% of Nabor Point observations and for 97% of Castlemartin observations. After quality control, the average percentage of observations with wave data somewhere in the coverage area was 86% for Nabor Point and 92% for Castlemartin. Two faulty units at Nabor Point, the main transmitter and the mains generator, lost 4.5% of observation time for waves during the period December 2003–May 2004. Dual radar wave data availability was consistently between 50% and 60% over the eight (or 32 allowing for contiguous cells) measurement cells which vary in average range (for the two radars) from 50 to 110 km offshore. Although there are no dual radar range cells at 150 km, the availability of single radar data is about 40% at this range.

The dual radar data availability in a particular cell is related to the product of the two single radar data availabilities for the appropriate ranges. This indicates that dual radar wave data availability at 150 km will be about 16%. A number of changes to increase availability of single radar data have been identified in this trial. These include changes to the host computer operating system, improved antenna control, and monitoring and power amplifier specifications.

III. Waves

The radar operating frequencies of less than 10 MHz provide both advantages and disadvantages. These frequencies are better at providing accurate wave information at high sea states [36], [37] but the ocean wave frequency range for which full inversions are possible has a lower high-frequency cutoff. This limited frequency range is important to take into account when comparing integrated parameters from the directional spectrum and, as will be shown in Section III-B, wave period is particularly sensitive to the frequency range. Another limitation is that the first-order Bragg-matched waves cannot be assumed to be fully developed wind waves in low sea states. The first-order Bragg-matched wave at 10 MHz is at 0.32 Hz. This is at the peak of a Pierson–Moskowitz spectrum with a waveheight of about 0.4 m. The inversion method used assumes that the Bragg-matched wave is far from the peak so a waveheight much greater than 0.4 m is needed. Also, in these conditions, higher second-order signal-to-noise ratio is required to make any wave measurements; no measurements are made when this signal-to-noise drops below 15 dB. Over the ten months of operations reported here, a lower limit of about 1 m significant waveheight has been identified below which wave measurement is increasingly inaccurate. In addition to these limitations, all related to the scattering model [38], [39] used in the measurements, interference levels, often associated with ionospheric propagation, are higher at low radio frequencies and can limit data availability and/or accuracy.

In this paper, we compare the radar wave measurements with those of a Datawell directional waverider deployed at position 4 on the map (Fig. 1), and with the U.K. Met Office wave model products at the same location. The buoy was deployed in January 2004, lost at the end of February 2004, and then recovered and

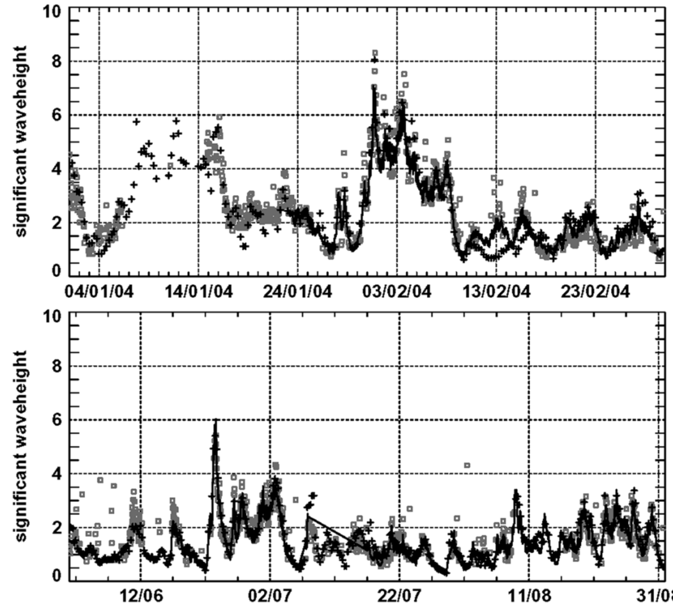

Fig. 2. Significant waveheight (m) comparisons for periods January–February 2004 and June–August 2004. Radar measurement "□," buoy measurement "—," and model "+."

redeployed in June 2004. Full resolution spectral data are available for the period to the end of February 2004, limited resolution spectral data (due to real time transmission limitations) for the later period. The comparisons of parameters evaluated over frequency ranges less than the full range are, therefore, likely to be subject to greater uncertainty in the data presented here for the summer period.

A. Waveheight

Significant waveheight is defined using the zeroth moment of the frequency spectrum $S(f)$, i.e.,

$$Hs = 4\sqrt{\int_{f_0}^{f_1} S(f)df}$$

where f_0 to f_1 is the frequency range of the measurement.

Fig. 2 shows the radar measurement of significant waveheight compared with the buoy and model data. There is reasonable agreement with occasional spikes in the radar data. The statistics of this comparison are presented in Table I. These show that during the earlier period when there were some high sea states, the agreement between buoy and radar is better, as measured by the correlation coefficient and ratios, than in the later predominantly low sea state period, although the mean and root-mean-square (rms) differences are similar in both periods. Comparing the model with the buoy for these two periods does not show this seasonal variation. In the first period, the model and radar perform similarly with the model doing marginally better in the second period. Fig. 3 shows how the waveheight is distributed in frequency. The agreement here (see, also, Table I) shows that the frequency spectra measured by radar and buoy are generally in good agreement. The difference in total waveheight statistics between the winter and summer periods seems to be manifested

TABLE I
COMPARISON OF SIGNIFICANT WAVEHEIGHT ESTIMATES FOR RADAR, BUOY, AND MODEL DATA. NO—NUMBER OF COTEMPORAL, COLLOCATED MEASUREMENTS; CC—CORRELATION COEFFICIENT; MEAN—MEAN DIFFERENCE IN METERS; RMS—ROOT-MEAN-SQUARE IN METERS; MEAN, SD%—MEAN AND STANDARD DEVIATION OF THE RATIO OF ESTIMATES

	January-February 2004						June-August 2004					
	no	cc	mean	rms	mean%	SD%	no	cc	mean	rms	mean%	SD%
Pisces/buoy	457	.94	.11	.57	2.5	22.7	491	.86	.06	.43	8.0	44.9
Pisces/Model	120	.9	-0.01	.6	4.7	36.3	108	.78	-0.08	.51	1.9	37.1
Model/Buoy	145	.96	0.09	.48	2.4	23.3	254	.94	.14	.3	12.1	20.6
Pisces/buoy NP	697	.82	-0.05	.74	7.2	38.5						
Pisces/buoy CM	688	.86	-0.12	.66	0.3	37.						
Pisces/buoy NP/CM	550	.86	-0.04	.64	3.7	33.1						
Pisces/buoy <0.1Hz	456	.94	.09	.45	34.9	72.7	479	.72	.21	.49	117.9	187.4
Pisces/buoy 0.1-0.2Hz	456	.92	.15	.48	9.8	27.4	479	.9	.12	.33	12.5	30.1
Pisces/buoy 0.2-0.3Hz	380	.63	-.17	.33	-19.	40.5	393	.55	-.14	.27	-17.4	34.6
Pisces/buoy peak	456	.88	0.	.4	1.8	34.1	479	.74	.01	.36	14.7	87.1

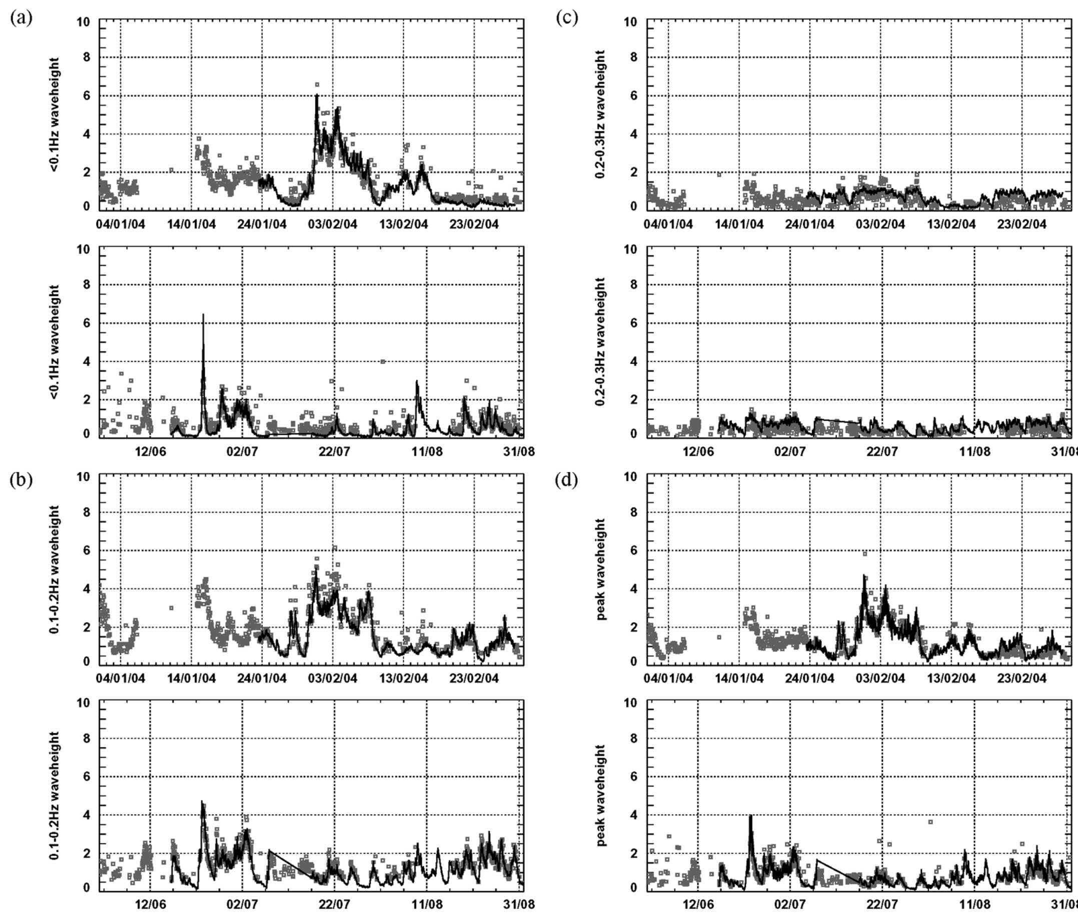

Fig. 3. Contributions to significant waveheight (m) for periods January–February (above) 2004 and June–August (below) 2004 from (a) <0.1 Hz, (b) 0.1–0.2 Hz, (c) 0.2–0.3 Hz, and (d) spectral peak. Radar measurement "□" and buoy measurement "—."

mainly at low ocean wave frequencies probably reflecting interference or ship signals which are more dominant in low sea conditions.

Estimates of waveheight are also available from each radar independently using simple empirical formulas relating integral properties of the radar Doppler spectrum to buoy measured waveheight [16]. When wave energy is propagating roughly perpendicular to the radar, the backscatter is lower than in the case where waves are roughly aligned with the radar. This leads to different empirical relationships for these two cases, so single radars provide two possible estimates of waveheight. At the intersection points of two radars, an unambiguous estimate of Hs can be obtained by comparing the two estimates from each of them. Fig. 4 shows plots comparing the buoy data with the individual radar estimates assuming no perpendicular propagation, the combined estimate, and the estimate obtained through inversion. The inversion estimate is the best in terms of the correlation coefficient and mean-square-error (mse) (see Table I). Although the quality criteria used to decide whether data are suitable for wave measurement are similar for the inversion and the single

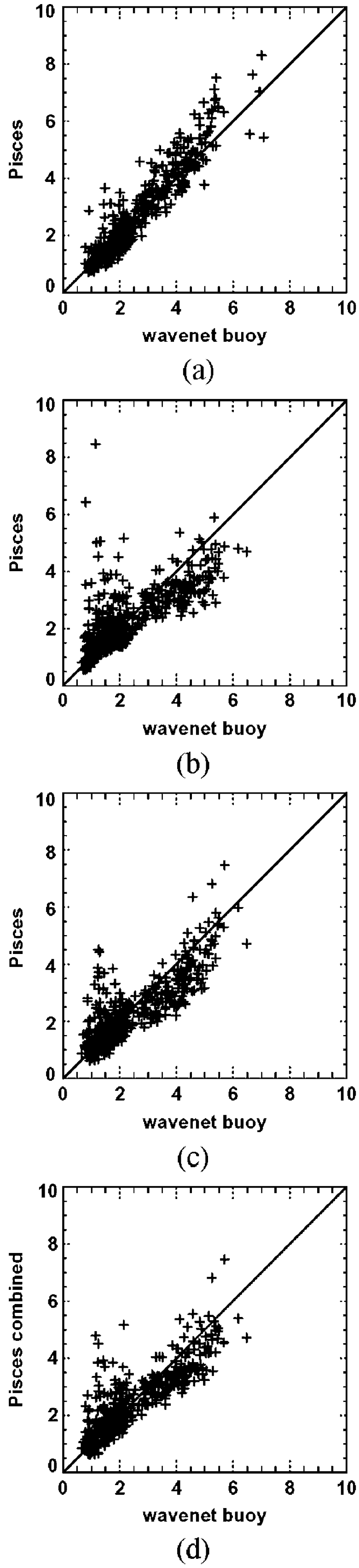

Fig. 4. Comparison of single and dual radar algorithms for Hs measurement (m). (a) Full inversion. (b) Single radar estimate from the Nabor Point site. (c) Single radar estimate from the Castlemartin site. (d) Estimate obtained by combining single radar estimates from both sites.

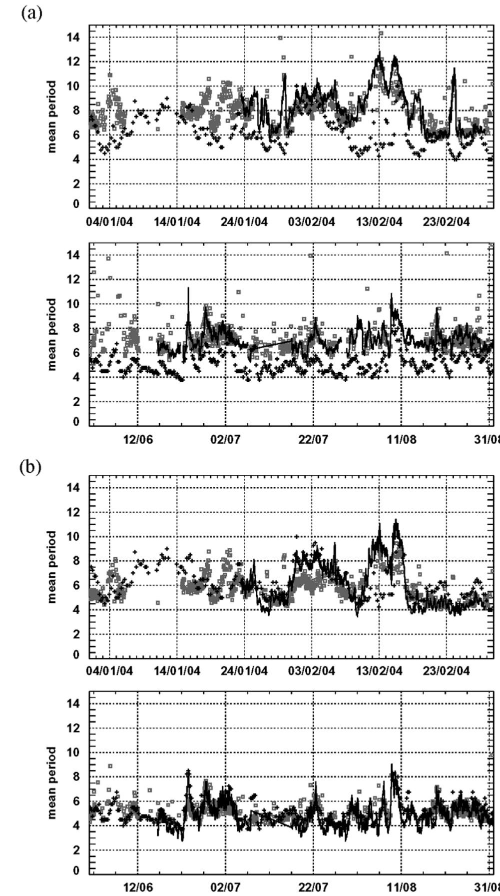

Fig. 5. Mean period (s) comparisons. Over the frequency range of (a) the radar measurement and (b) the buoy measurement. Buoy measurement "—," radar measurement "□," and model (no frequency range adjustment) "+."

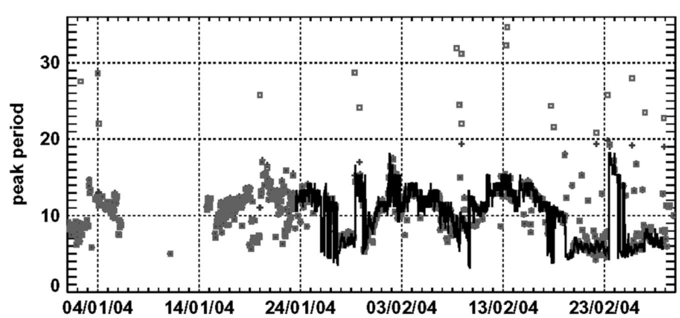

Fig. 6. Winter peak period (s) comparisons. Radar measurement "+," radar measurement confined to frequencies >0.05 Hz "□" (note these are mostly superimposed), buoy measurement "—."

radar estimates, combining the latter provide rather more measurements because the inversion data have an additional post-processing criterion imposed to remove data where inversion convergence was poor.

B. Wave Period

Mean period is obtained using either the first or second moment of the frequency spectrum $S(f)$, i.e.

$$T_n = \left(\frac{\int_{f_0}^{f_1} S(f)df}{\int_{f_0}^{f_1} f^n S(f)df} \right)^{\frac{1}{n}}.$$

TABLE II
COMPARISON OF PERIOD ESTIMATES

	January-February 2004				June-August 2004			
	no	cc	mean	rms	no	cc	mean	rms
Pisces/Model	120	.05	1.55	2.27	108	.07	1.65	2.18
Pisces/buoy Tz	457	.59	1.73	2.26	491	.14	2.08	2.58
Pisces to 0.58Hz/buoy Tz	457	.74	-.38	1.23	491	.48	.09	.84
Pisces/buoy to 0.22Hz	456	.79	-.21	1.05	479	.38	.22	1.27
Model/Buoy	145	.66	1.55	2.27	254	.81	.42	.72
Pisces/Buoy Tpeak	457	.5	.56	3.82	478	.13	1.05	4.56
Pisces/Buoy Tpeak >0.05	457	.7	.15	2.42	478	.22	.53	3.06
Pisces/Buoy Tz Hs>2m	265	.82	1.04	1.31				

Here, we compare the second moment which is sometimes referred to as the zero-crossing period since this is the quantity provided from the wave buoy and the model. For the buoy, the integration range is from about 0.05 to 0.58 Hz, whereas the radar measurements are limited to just over 0.22 Hz with a variable lower limit dependent on the quality of the radar Doppler spectrum. When assessing wave period measurements, it is important to take into account the frequency range used. We have, therefore, recalculated the buoy parameters to 0.22 Hz and also removed frequencies <0.05 Hz in the radar data. We have also added a f^{-5} tail to the radar data to extend it to the buoy limit and calculated the corresponding period for this range. Fig. 5(a) and (b), respectively, and Table II show the results. These results demonstrate the importance of accounting for differences in frequency range. Much better agreement is obtained when the same frequency range is used.

Peak periods for the winter period are compared in Fig. 6 and Table II. Here, it can be seen that limiting the frequency range to >0.05 Hz removes some but not all of the noisy peaks in the radar data (see related discussion in Section III-D). For the summer data set, where peak frequencies are generally higher, the impact is lower as can be seen in Table II.

C. Wave Direction

Mean wave direction ϑ is determined from the frequency and direction spectrum ($S(f)$ and $\theta(f)$, respectively) using

$$\tan\vartheta = \frac{\int_{f_0}^{f_1} \sin\theta(f) S(f) df}{\int_{f_0}^{f_1} \cos\theta(f) S(f) df}.$$

This formula can be used to estimate a peak direction using, in the case for the radar measurement, frequencies (f_0 to f_1) within 10 mHz of the spectral peak. $S(f)$ and $\theta(f)$ are both determined from the directional spectrum $S(f,\theta)$ and $\theta(f)$ is rather more sensitive to noise in that spectrum than $S(f)$.

Fig. 7 shows that the accuracy of ϑ depends on waveheight with much better estimates for waveheights greater that about 2 m. The reason for this is that at lower waveheights any spurious features in the spectrum generated by noise (for example a ship or interference) in the radar signal will have a greater impact on this parameter than on waveheight itself (see also discussion in Section III-D). The statistics of the direction comparisons are presented in Table III.

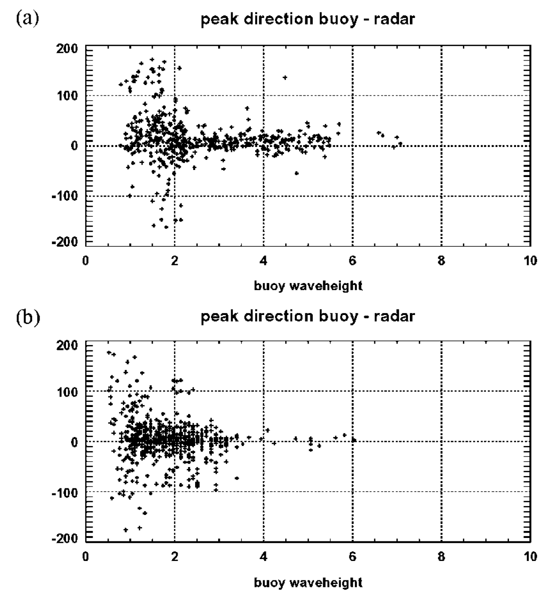

Fig. 7. Difference between buoy peak direction and radar peak direction (vertical axis in degrees) compared with waveheight (m) for the two periods: (a) January–February 2004 and (b) June–August 2004.

D. Directional Spectrum

Previous work [40], [33] has demonstrated the value of looking at the frequency and directional spectrum to understand the main differences between the radar parameters and those measured by the buoy. The full directional spectrum can indicate reasons for particular differences at particular times but, as yet, there is no accepted method of comparing these on average. For this experiment, we do not (yet) have the second-order Fourier coefficients for the buoy that would have enabled detailed case-by-case comparisons. However, differences in mean frequency spectra, in mean spectral ratios (a value of 1 being perfect agreement), and in mean direction spectra (i.e., mean directions at each frequency) do provide additional information to explore further the parameters results presented previously.

Fig. 8 shows these means for February 2004. Fig. 8(a) includes all the data and the mean spectral ratio is very large below about 0.08 Hz. There is also a large direction difference below about 0.06 Hz. The averages in Fig. 8(b) include only energy at and above the frequency of the spectral peak in the buoy data. Mean spectral ratios are now much better (i.e., closer to 1), although there is still an increased error below about 0.08 Hz. Direction differences are below 10° over most of the frequency

TABLE III
COMPARISONS OF DIRECTION ESTIMATES

	January-February 2004				June-August 2004			
	no	cc	mean	rms	no	cc	mean	rms
Pisces/Model peak	120	.43	-9.49	44.12	108	.48	-1.13	35.75
Model/Buoy	145	.72	-4.82	33.86	254	.68	.08	26.38
Pisces/buoy peak	457	.42	-13.61	47.04	492	.48	-6.83	42.2
Pisces/buoy mean	457	.57	-11.56	36.62	491	.6	-4.52	33.38
Pisces/buoy <0.1Hz	456	.17	-6.21	47.71	479	.13	-6.92	66.1
0.1-0.2Hz	456	.55	-12.93	41.72	479	.62	-2.69	30.51
0.2-0.3Hz	380	.45	-14.19	52.97	393	.45	-1.12	49.48
Pisces/buoy peak Hs>2m	265	.66	-8.08	26.8				

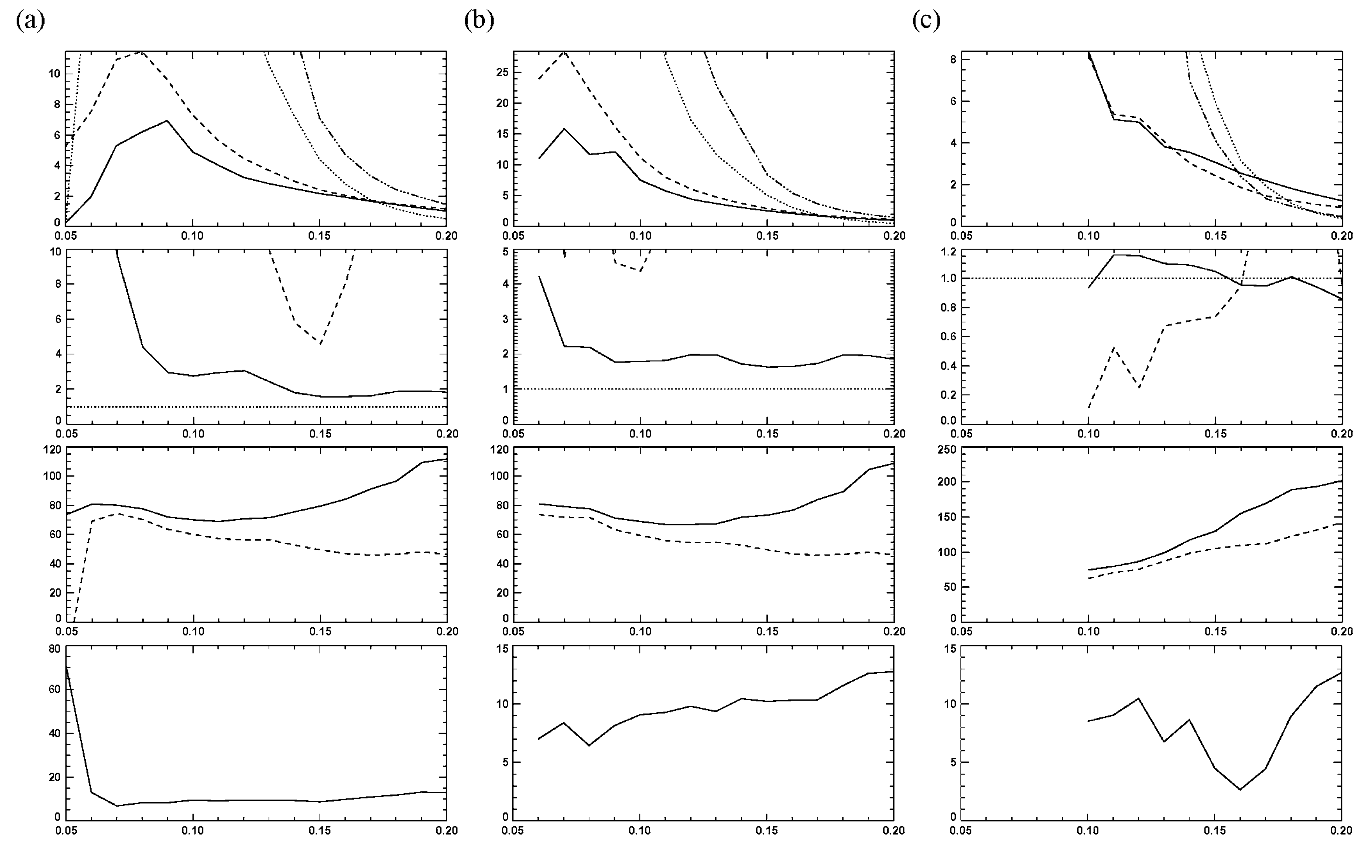

Fig. 8. From top to bottom: mean frequency spectrum (m^2/Hz), mean spectral ratio (horizontal dashed lines at a ratio of 1), mean direction (°), and mean direction difference (°). Solid is buoy data and dashed is the radar. Dot and dash–dot in the top row graphs are the corresponding variances. (a) All data. (b) Excluding values below the buoy spectral peak. (c) Including only cases where the buoy peak is <0.1 Hz.

range and are slightly lower at the low frequencies. The reduced errors in Fig. 8(b) show that the main differences can be associated with noise generating spurious low-frequency components below the spectral peak. Fig. 8(c) includes only those cases where the buoy spectral peak was at a frequency >0.1 Hz. Both amplitude and direction now agree well confirming that it is the lower ocean wave frequencies that are most susceptible to noise. Previous comparisons of this kind [40], [33] were for data measured at high radio frequencies and in conditions where the mean spectral peak was above 0.1 Hz. For those cases, comparisons were rather similar to those shown in Fig. 8(c) here.

In [41], we noted two conditions where there was the largest difference between the single radar measurements and the U.K. Met Office model outputs. These were fetch-limited wave development and swell-dominated seas. Both of these situations occurred during February 2004 when we also have the buoy data for comparison so we will examine these occasions here in more detail. Fig. 2 shows the waveheights during this period.

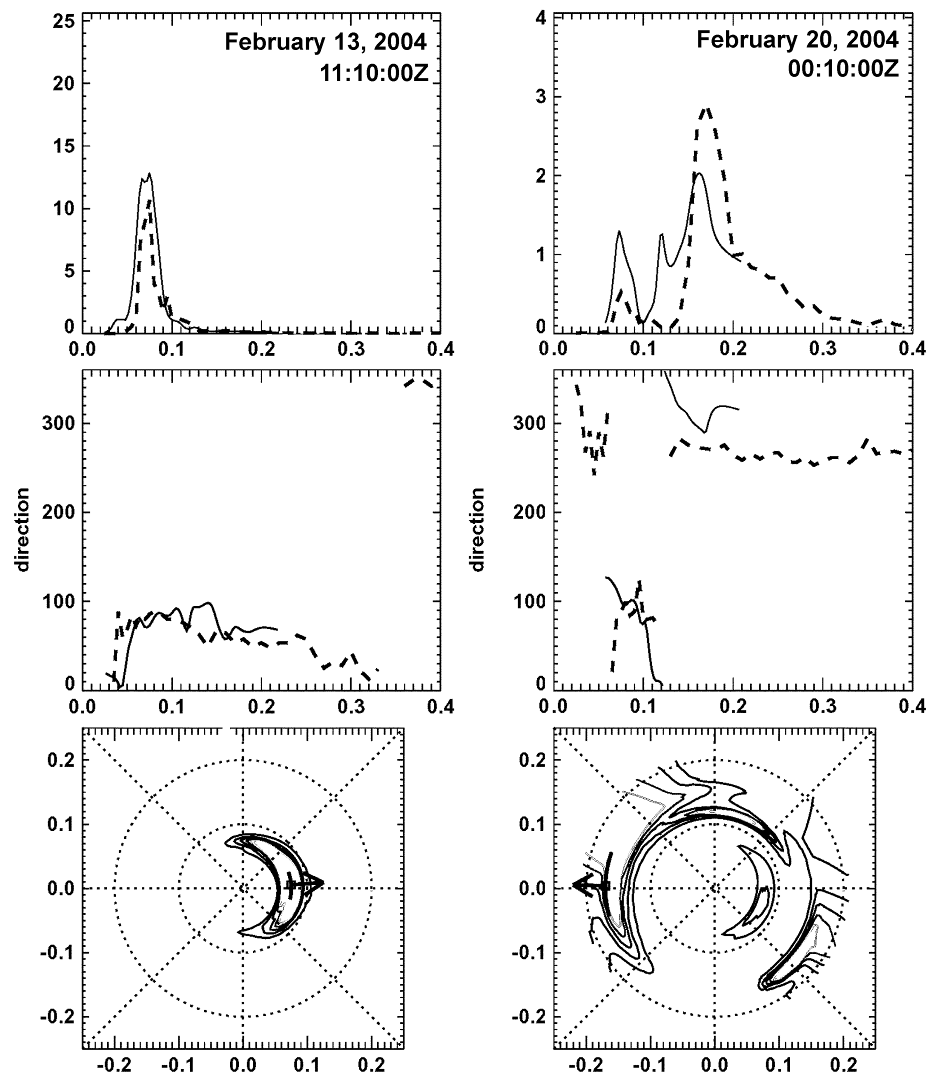

Fig. 9. Top panel—frequency spectra (solid is the radar and dashed is the buoy). Middle panel—mean direction versus frequency. Bottom panel—directional spectrum with contours at intervals of and with the lowest level at 0.1* peak amplitude. The arrow in the lower panel shows peak amplitude and frequency as measured by the buoy. (a) Swell dominated on February 13, 2004. (b) Mixed wind sea and swell on February 20, 2004.

Between February 11–17, 2004, the dual-radar and buoy waveheights are similar and are significantly higher than the model waveheight. There is not much radar data on February 11 and 12, 2004, but there is plenty in the period February 13–16, 2004, which was characterized by swell with peak frequency in the range 0.07–0.08 Hz propagating from just south of west [see Fig. 9(a)]. The model, buoy, and radar peak directions are in reasonable agreement during this period. These results together with the previous work do suggest a problem with swell-dominated seas in the Met Office wave model.

From February 20 to February 21, 2004, the situation is very different. Here, the dual-radar and buoy waveheights are again similar but now the model waveheights are slightly higher. The radar and buoy directional spectra show fetch-limited wind waves peaking at 0.15–0.2 Hz with some evidence of a smaller swell component peaking at 0.08–0.09 Hz [see Fig. 9(b)]. Winds were blowing from the east. Comparing these data 30 km further offshore (not shown), an increase in dual-radar waveheight closer to the model height is found, although the radar heights are noisier at this range. Even though the differences in waveheight are small, there is some indication here of a problem with fetch-limited growth in the Met Office model. The case that was discussed in [41] was in stronger offshore wind conditions and, hence, was more pronounced.

IV. Surface Currents

A. Tides

The current data for each cell for the six-month period December 2003 to May 2004 were analyzed for tides with a least-squares harmonic analysis program fitting 16 constituents -12, which can be calculated for a month's data—O_1, K_1, μ_2, N_2, M_2, L_2, S_2, MN_4, M_4, MS_4, M_6, and $2MS_6$ and a further four requiring six-months data—$2N_2$, ν_2, λ_2, and K_2—plus the mean (Z_0). Such analysis has no difficulty treating data with gaps which are common with HF radar data. Although the dynamics of the Celtic Sea away from the coasts is dominated by

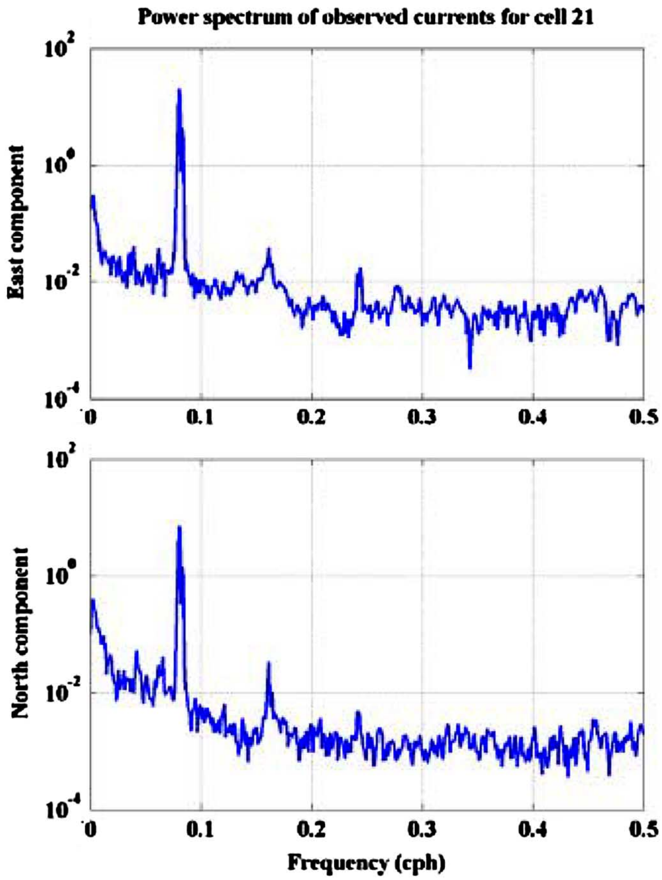

Fig. 10. Power spectra [in $(m/s)^2$ per cycle per hour (cph)] for the observed radar currents for cell 4.

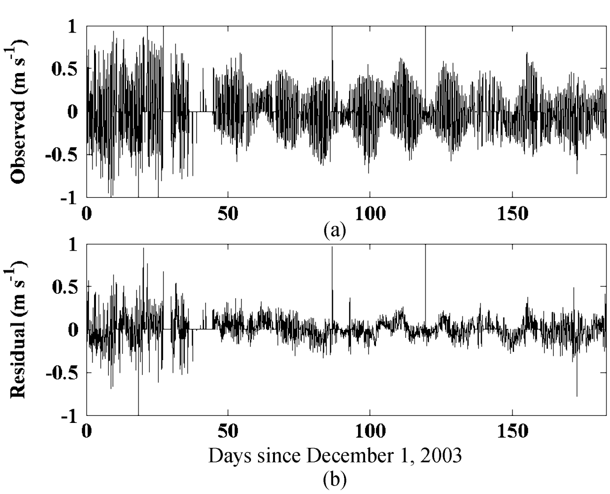

Fig. 11. East component for cell 2 for the observed (a) radar data and (b) tidal residual.

the semidiurnal tides (particularly the M_2, S_2, N_2, and K_2 constituents), the diurnal, fourth, and sixth diurnals were included as a check on the quality of the data. No problems with the data were detected. For instance, see the spectra in Fig. 10, which shows the dominance of the semidiurnal band [about 0.08 cycles per hour (cph)] and a small amount of tidal energy in the fourth-diurnal band (about 0.16 cph) in the north component and even less in the sixth-diurnal band. There was very little energy

TABLE IV
M_2 TIDAL ELLIPSES FOR THE HF RADAR DATA

Cell	Maximum amplitude (m s^{-1})	Minimum amplitude (m s^{-1})	Phase (°)	Direction (°)
11	0.39	0.17	-95	67
12	0.30	0.13	-89	68
13	0.36	0.01	-81	18
21	0.38	0.22	-105	80
22	0.37	0.22	-125	116
23	0.30	0.19	-150	161
31	0.50	0.14	-102	83
32	0.43	0.19	-123	111
33	0.49	0.13	-133	130

TABLE V
M_2 TIDAL ELLIPSES FROM A DEPTH-AVERAGED NUMERICAL MODEL. THE PHASES ARE NOT DIRECTLY COMPARABLE WITH THOSE IN TABLE IV SINCE THEY ARE TO DIFFERENT TIME ORIGINS, ALTHOUGH THEIR RELATIVE MAGNITUDES ARE

Cell	Maximum amplitude (m s^{-1})	Minimum amplitude (m s^{-1})	Phase (°)	Direction (°)
11	0.41	0.13	106	67
12	0.31	0.09	116	62
13	0.28	-0.06	107	66
21	0.43	0.20	100	77
22	0.34	0.24	91	97
23	0.29	0.18	-3	205
31	0.53	0.18	79	108
32	0.56	0.24	65	120
33	0.63	0.23	53	141

at diurnal frequencies but significant energy at low frequencies. (Once a tidal analysis is calculated, the nontidal residuals can be determined and regular time series constructed by filling the gaps in the observations with the predicted tidal currents and in the residuals with the mean value. Meaningful spectra can then be calculated.)

As for any current measurement in an area dominated by tides, the quality of the data can often be checked by looking at the tidal residuals, particularly for consistency and timing errors. For instance, for this deployment Fig. 11 shows for cell 2 (see Fig. 1) large residuals during December 2003. Initial thoughts were that this might be a timing problem of order an hour but it transpired to be beam-steering problem affecting one beam which was corrected in January 2004.

The quality of the data is also shown in Table VI in three ways—the goodness of the tidal analysis, for instance, in the percent variance of the residual relative to the observed data, the (low, except for cell 3 where the number of spikes represents 12% of the record) number of large spikes, and the noise levels. The noise levels were calculated from the average spectral energy in the residuals in the frequency band 0.4-0.5 cph—Fig. 10 indicates that this level is reached for frequencies higher than 0.25 cph. The noise levels are equivalent to an average vector standard deviation of 0.06 m s^{-1}. Highest noise levels were at cells 6, 7, and 9, about twice the average. (The frequency resolution of the radar Doppler spectra is equivalent to a nominal current speed resolution of 0.092 m s^{-1}, but this is improved by fitting a quadratic to the peak and neighboring points.) All estimates indicate that the current data in cell 3 are of no value.

TABLE VI
VARIOUS ESTIMATES OF THE QUALITY OF THE HF RADAR CURRENT MEASUREMENTS

Cell	SD observations (ms^{-1})	SD residuals ($m\ s^{-1}$)	% variance in residuals	Number of spikes	East component noise (m^2s^{-2})/cph	North component noise ($m^2\ s^{-2}$) / cph
11	0.36	0.14	15	7	0.0010	0.0018
12	0.31	0.17	30	7	0.0027	0.0044
13	1.16	1.11	92	115	0.0253	0.1885
21	0.37	0.14	15	3	0.0038	0.0014
22	0.37	0.16	19	1	0.0025	0.0040
23	0.33	0.19	32	8	0.0015	0.0102
31	0.46	0.22	23	3	0.0111	0.0035
32	0.40	0.15	15	3	0.0030	0.0033
33	0.44	0.20	22	6	0.0032	0.0 099

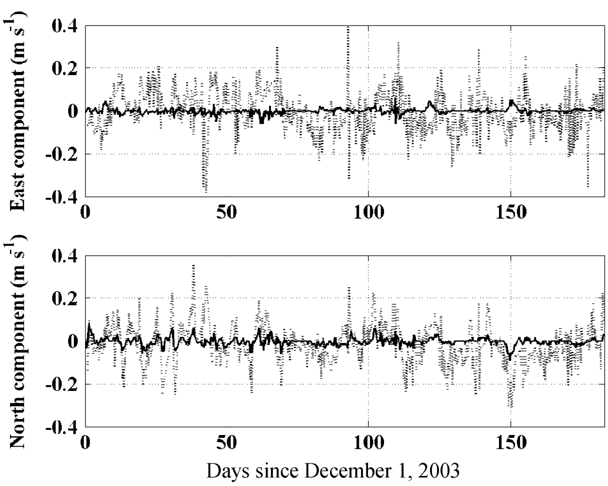

Fig. 12. Time series of residual currents for cell 4—"- - -" radar; "—" depth-averaged model.

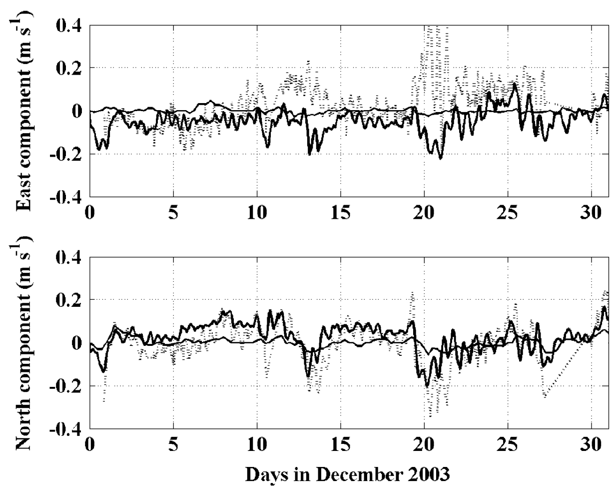

Fig. 13. Comparison between estimates of the tidal residual current for cell 4 for December 2003 from the radar (- - -), hourly surface currents from a 3-D model (—) and 6-h depth-averaged model currents (—).

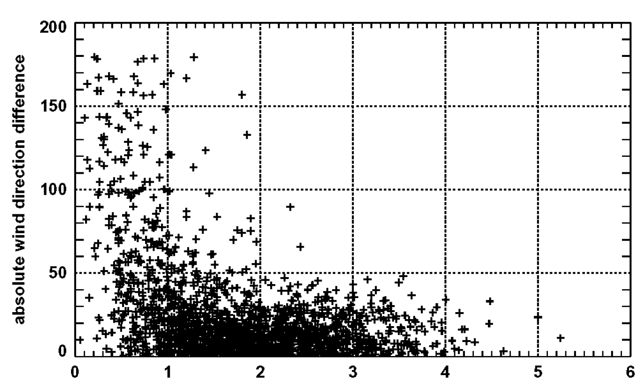

Fig. 14. Magnitude of the difference in wind direction between HF radar and model against the ratio of Bragg frequency to a wind-speed-dependent peak frequency.

The calculated constituents were compared with a Proudman Oceanographic Laboratory (POL), Liverpool, U.K., two-dimensional (2-D) (depth-averaged) shelf-wide tidal model with a 12-km grid (Tables IV and V). The general agreement is good except for cells 8 and 9 where the observations indicate weaker M_2 currents than are predicted by the model. Perhaps the model is overpredicting here since this region, near St. David's Head and at the junction between the Bristol and St. George's Channels and the Celtic Sea, has significant tidal gradients. It is hard to see why there should be spatial variations in the quality of the tidal currents measured by the radar. Further work is needed to investigate the difference. An element of caution should accompany a comparison between depth-averaged (model) and surface (radar) tidal currents since although tidal currents usually vary little in the upper half of the water column some variation is expected, for instance, in the shape and sense of rotation of the tidal ellipse which may account for the differences in the minimum amplitude values.

B. Residuals

The calculated tidal residuals were compared with depth-averaged model surge currents included in the wave model output. A quick assessment of Fig. 12 showed that the comparison was not really meaningful since the time resolution of the model currents (6 h) was too slow and since more processes force surface currents (for instance, the direct response to wind forcing, depth variation in return flows) than the depth-averaged currents. Despite this, there are clearly times when the two are related, although the surface radar currents are much stronger than the depth-averaged model currents.

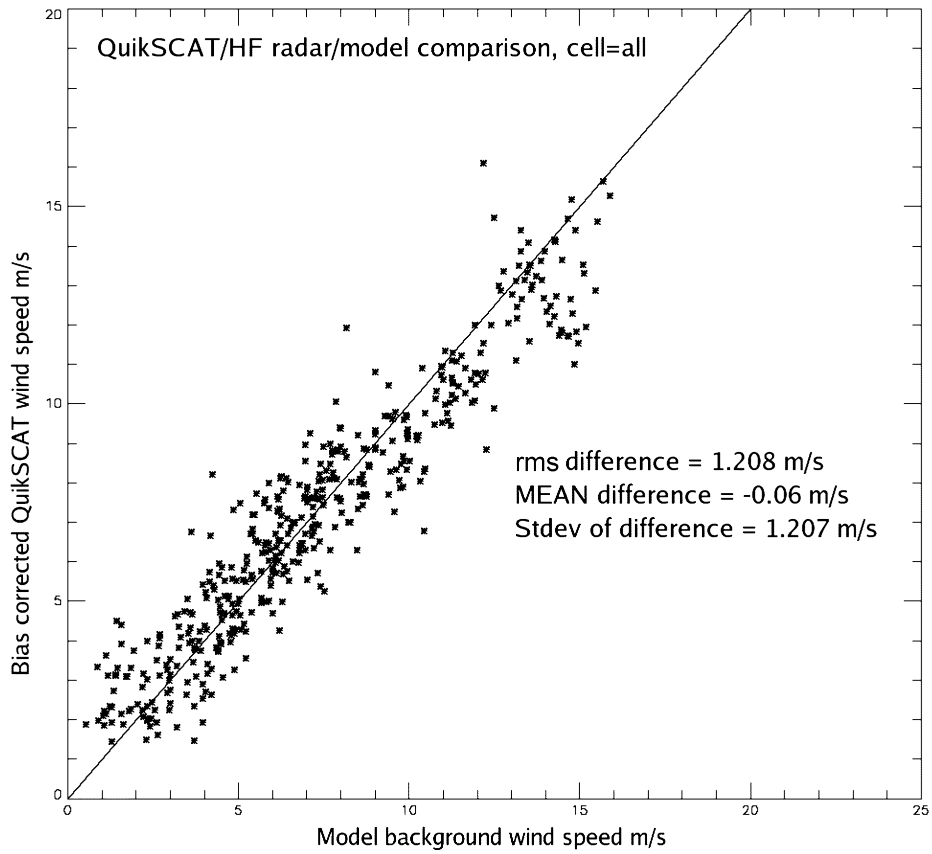

Fig. 15. Comparison of bias corrected QuikSCAT data and model background wind speeds for all cells.

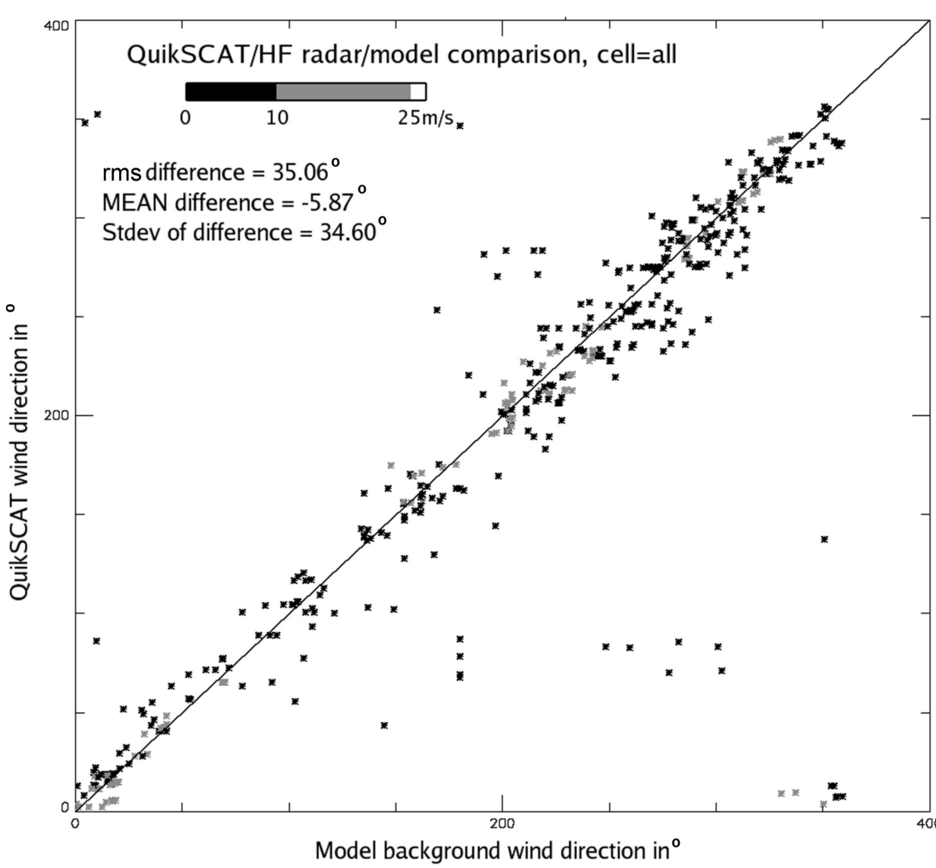

Fig. 16. Comparison of QuikSCAT and model background wind directions. Color indicates model background wind speeds.

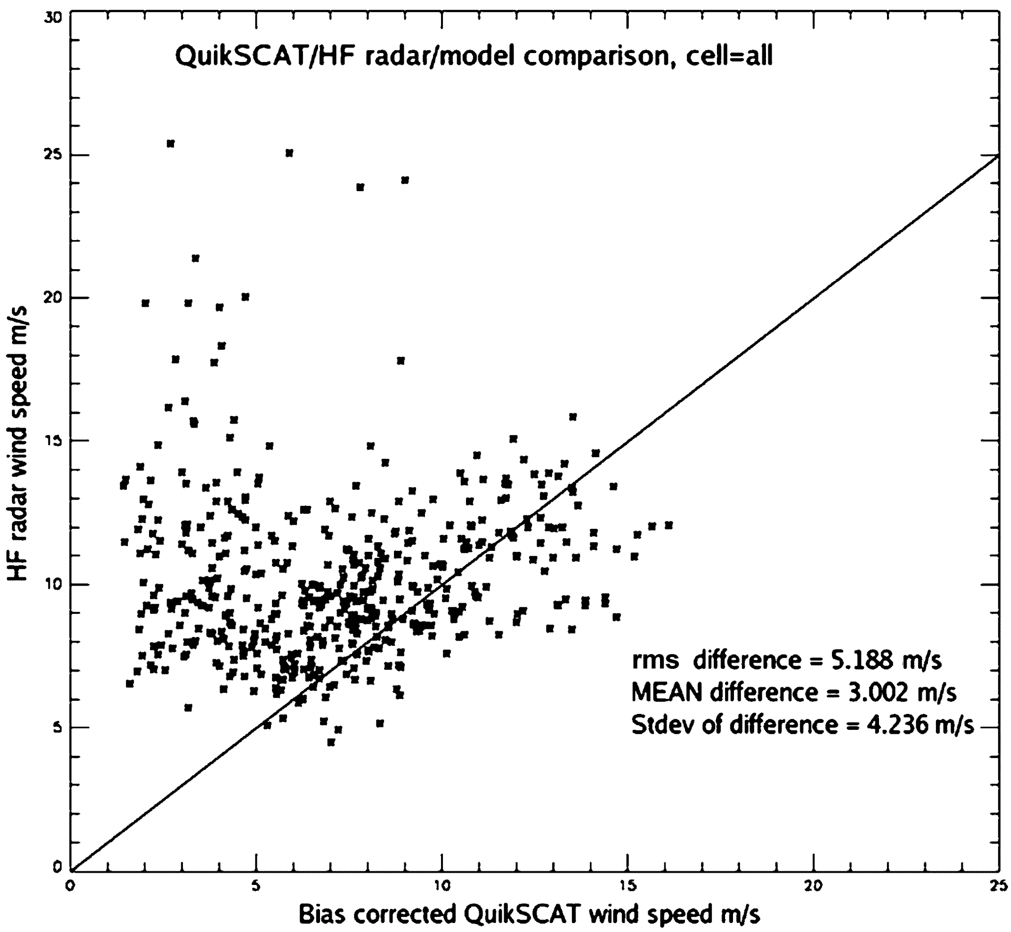

Fig. 17. Comparison of HF radar and bias corrected QuikSCAT wind speeds for all cells. HF radar reports almost no wind speeds less than 5 m/s.

Comparisons with surface currents from a three-dimensional (3-D) model are essential. Fig. 13 shows preliminary results for hourly surface radar and 3-D model tidal residual currents and 6-h depth-averaged model currents, for December 2003. Comparisons between the radar and 3-D model surface residual currents for the different cells gave correlation coefficients between 0.45 and 0.68, with model and radar speeds having a similar magnitude. The differences suggest that as much may be learned about the model's accuracy from this as the radar's, for instance, the agreement between the radar estimates (dashed line) and the model predictions (solid line) in Fig. 13 is good for the north component and worse for the east component.

V. Winds

We are investigating two approaches for wind speed measurement. One makes use of a simple wind wave model [42]. This method was used for this data set but is not good in low seas because then waveheight is often swell rather than wind sea dominated. The second approach involves seeking empirical relationships between features in the radar Doppler spectrum and a locally measured wind speed [43]. Results are promising but require a data set with offshore wind speed measurements to develop a robust algorithm.

Radar wind direction estimates are more robust. These are obtained using the ratio of the two first-order Bragg peaks and a model of short-wave directional spreading [30]. The assumption is made that the ocean waves responsible for first-order scatter are locally generated wind waves propagating in the direction of the wind. This assumption will be valid for waves at frequencies much higher than the wind wave peak but becomes less so closer to and below this peak. This can be seen clearly in Fig. 14, which shows the difference between radar and model wind direction as a function of the ratio of the first-order Bragg frequency to the peak frequency expected for fully developed wind waves using the Pierson–Moskowitz model (see, for example, [44]). As this ratio approaches and drops below 1, the errors in wind direction estimation are larger. When we have a robust wind speed algorithm, it will be possible to flag such data and also provide advice to the radar operator to increase radio frequency where possible. Unfortunately, significant waveheight, which we can measure, does not provide a good proxy for wind speed at low wind speeds because of the influence of swell.

HF radar wind data have also been compared with QuikSCAT for the period of January 27, 2004–July 31, 2004 ($\sim$6 months). The QuikSCAT data were processed (but not thinned) using only data from the "sweet" part of the swath that has passed quality control tests (e.g., for rain contamination) as outlined in [45]. QuikSCAT match up points have a footprint of $\sim$25 km, while HF radar points have a range resolution of $\sim$15 km, so some differences may be attributed to spatial variations in the

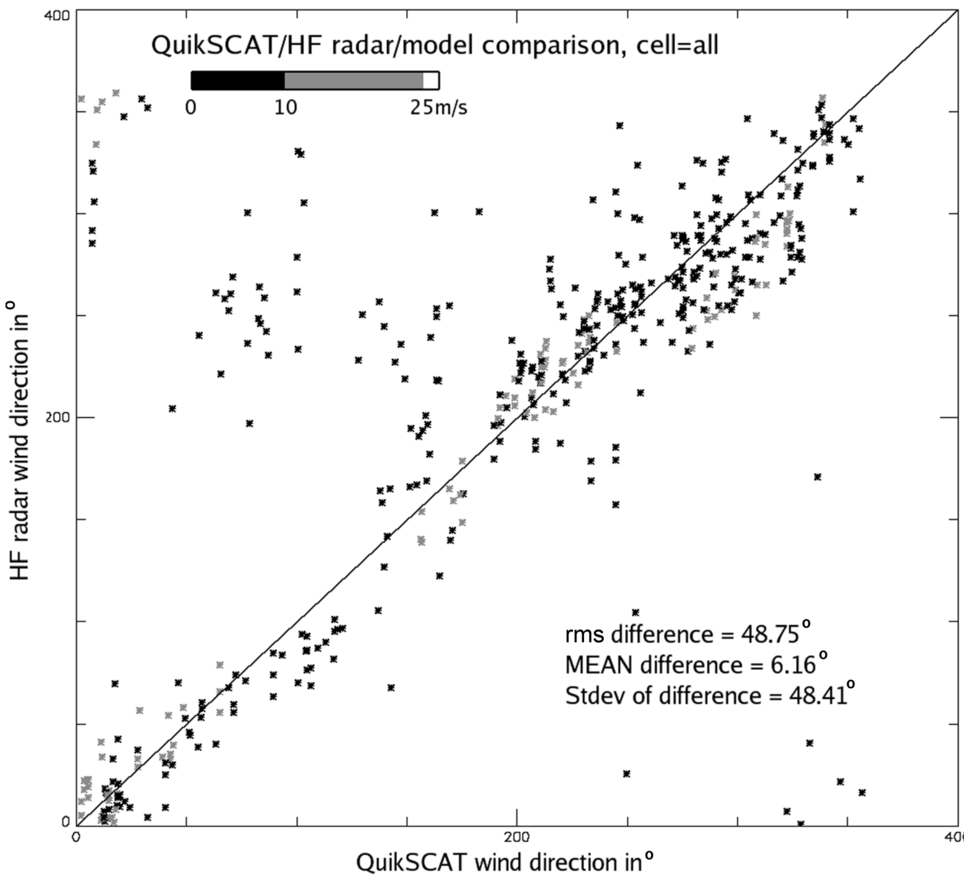

Fig. 18. Comparison of HF Radar and QuikSCAT wind directions. Color online indicates QuikSCAT wind speeds.

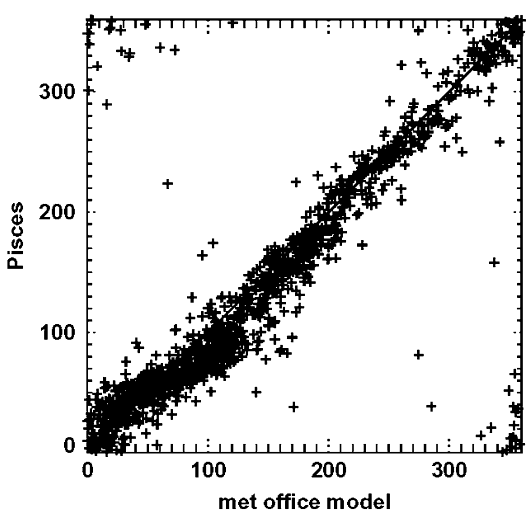

Fig. 19. Scatter plot of radar against model wind directions (in degrees) using the Bragg to wind-speed-dependent peak frequency criterion.

TABLE VII

WIND DIRECTION COMPARISONS. NOTE THAT THE PISCES/MODEL COMPARISONS WERE FOR THE PERIOD DECEMBER 2003–AUGUST 2004 AT CELL 4. THE QUIKSCAT COMPARISONS ARE FROM JANUARY 2004 TO JULY 2004 AND INCLUDE DATA FROM CELLS 1, 2, 4, 5, AND 6

	N	Correlation coefficient	Mean difference	rms	Standard deviation
Pisces/model	915	.66	-8.35	43.11	43.32
Pisces/ /QuikSCAT	462		6.16	48.75	48.41
QuikSCAT/ model	462		-5.87	35.09	34.61
Pisces/model with Bragg condition	648	.89	-7.91	23.13	21.75

wind field on these scales. The QuikSCAT fields were also compared with the Met Office model and show good agreement (see Figs. 15 and 16). Comparisons of wind speed (see Fig. 17) show clearly the problem with the radar wind speed estimate in low wind conditions. The wind direction comparisons (see Fig. 18) show the problems in low wind speed cases discussed previously. Fig. 19 shows a scatter plot of wind directions (for all radar and coincident model winds during the period December 2003– August 2004) using the model wind speeds to remove data below a threshold of Bragg:peak frequency of 1.1, as discussed previously, to show the potential improvement in accuracy of the measurement. The statistics of the wind direction comparisons are summarized in Table VII, where it can be seen that, using the Bragg threshold, the radar data compares as well as, if not better than, QuikSCAT with the model.

The same Bragg threshold was also used to investigate errors in the wave measurements since the inversion assumes that short waves, i.e., waves of the same order as the Bragg matched waves, are wind driven and aligned with the wind. However, the dependence on waveheight itself for period and direction estimates was much clearer.

VI. Summary and Future Prospects

The trial began in December 2003 and continued until June 2005. Detailed comparisons with the buoy and model data are continuing. We have not found any data sets that change the main conclusions presented here. We do have a few more large (>6 m) waveheight events to explore in more detail.

The main conclusions are as follows:

- Significant waveheight can be measured with useful accuracy (e.g., mean difference and standard deviation with the buoy of 2.5% and 22.7% compared to the corresponding model values of 2.4% and 23.3% during January/February 2004) above a lower limit (at these operating frequencies) of about 1 m. For comparison, we note that according to the Datawell website (http://www.datawell.nl/), the wave buoy is accurate to 0.5% of the measured value.
- Wave period measurements need to be accompanied by information on the frequency range used. At the radar operating frequencies used in this paper, the maximum measurable ocean wave frequency is about 0.22 Hz.
- Peak and mean wave direction and period measurements are more accurate when waveheight is above about 2 m. Below this, spurious features in the directional spectrum sometimes contaminate the parameter estimates. The peak direction rms difference for waveheights >2 m was 26.8° during January/February 2004 and this compares well to the model rms difference of 33.9°.
- Directional spectra can be contaminated at low frequencies by noise (interference or ships). The higher frequency parts of the spectrum generally show good agreement.
- Dual radar current data at the cell location furthest from the two radars was not found to be useful. This cell was over 200 km from each radar. However, comparisons of single radar radial currents (not presented here) do show reasonable agreement with model currents to ranges near 200 km. The radar can be configured to get data at longer ranges if required. The other cells were all within 120 km and for these the currents were found to compare well with model currents especially when 3-D model currents were used.
- Wind speed is not yet an accurate measurement with HF radar. We have shown that accurate wind directions are possible when the first-order Bragg waves can be expected to be locally wind-driven.
- Although there were gaps in the dual radar data when both radars did not yield spectra of adequate quality at the measurement cell, single radar data in the overlap area were available from one or other (or both) radars more than 99% of the time. Methods of maximizing the use of these data are being evaluated.

One technique we are exploring to reduce the vulnerability of the parameter estimates to low-frequency noise is to partition the directional spectra and discard contributions that are not sufficiently continuous in space and time (which we expect to be noise-generated). The partitioning will also aim to separate and identify swell and wind sea contributions to the spectrum.

This paper has provided further evidence of the ability of HF radar systems to provide operational wave, current, and wind measurements in coastal regions. Discussions on the future role of HF radar in the United Kingdom wave monitoring network (WAVENET) are ongoing. At the time of writing, proposals were being considered for radars in two new locations on the English coast. If these go ahead they are likely to provide data for several years providing an invaluable opportunity for new algorithm development. More importantly, the availability of real-time simultaneous long-term wave current and wind data will be increasingly exploited by the coastal engineering and science communities to improve models, forecasts, and designs.

Acknowledgment

The authors would like to thank the contributions of all the Neptune Radar Ltd. staff who have worked at the radar sites. The buoy data have been provided by Centre for Environment, Fisheries and Aquaculture Science (CEFAS).

References

[1] H.-H. Essen, K.-W. Gurgel, and T. Schlick, "On the accuracy of current measurements by means of HF radar," *IEEE J. Ocean. Eng.*, vol. 25, no. 4, pp. 472–480, Oct. 2000.

[2] ——, "Comparison of remotely measured and modelled currents in coastal areas of Norway and Spain," *Global Atmos. Ocean Syst.*, vol. 9, pp. 39–64, 2003.

[3] H. C. Graber, B. K. Haus, R. D. Chapman, and L. K. Shay, "HF radar comparisons with moored estimates of current speed and direction: Expected differences and implications," *J. Geophys. Res.-C*, vol. 102, pp. 18 749–18 766, 1997.

[4] D. Prandle, "A new view of near-shore dynamics based on observation from HF radar," *Progr. Oceanogr.*, vol. 27, pp. 403–438, 1991.

[5] D. Prandle and D. K. Ryder, "Measurement of surface currents in Liverpool Bay by high-frequency radar," *Nature*, vol. 315, pp. 128–131, 1985.

[6] L. K. Shay, H. C. Graber, D. B. Ross, and R. D. Chapman, "Mesoscale ocean surface current structure detected by high-frequency radar," *J. Atmos. Ocean. Technol.*, vol. 12, pp. 881–900, 1995.

[7] B. M. Emery, L. Washburn, and J. A. Harlan, "Evaluating radial current measurements from CODAR High-Frequency radars with moored current meters," *J. Atmos. Ocean. Technol.*, vol. 21, pp. 1259–1271, 2004.

[8] J. T. Kohut, S. M. Glenn, and R. J. Chant, "Seasonal current variability on the New Jersey inner shelf," *J. Geophys. Res.*, vol. 109, 2004.

[9] D. Prandle, "Tidal and wind-driven currents from OSCR," *Oceanogr.*, vol. 10, pp. 57–59, 1997.

[10] E. D. R. Shearman and M. D. Moorhead, "Pisces: A coastal ground-wave radar for current, wind and wave mapping to 200 km ranges," in *Proc. IEEE Int. Geosci. Remote Sens. Symp. (IGARSS)*, 1988, pp. 773–776.

[11] B. J. Lipa and D. E. Barrick, "Least-squares methods for the extraction of surface currents from CODAR crossed-loop data: Application at ARSLOE," *IEEE J. Ocean. Eng.*, vol. OE-8, no. 4, pp. 226–253, Oct. 1983.

[12] K.-W. Gurgel, G. Antonischki, H.-H. Essen, and T. Schlick, "Wellen Radar (WERA): A new ground-wave HF radar for ocean remote sensing," *Coastal Eng.*, vol. 37, pp. 219–234, 1999.

[13] D. E. Barrick, "Extraction of wave parameters from measured HF radar sea-echo Doppler spectra," *Radio Sci.*, vol. 12, pp. 415–424, 1977.

[14] L. R. Wyatt, "Significant waveheight measurement with HF radar," *Int. J. Remote Sens.*, vol. 9, pp. 1087–1095, 1988.

[15] H. C. Graber and M. L. Heron, "Wave height measurement from HF radar," *Oceanogr.*, vol. 10, pp. 90–92, 1997.

[16] L. R. Wyatt, "An evaluation of wave parameters measured using a single HF radar system," *Can. J. Remote Sens.*, vol. 28, pp. 205–218, 2002.

[17] B. J. Lipa, "Derivation of directional ocean-wave spectra by inversion of second order radar echoes," *Radio Sci.*, vol. 12, pp. 425–434, 1977.

[18] B. J. Lipa, "Inversion of second-order radar echoes from the sea," *J. Geophys. Res.-C*, vol. 83, pp. 959–962, 1978.

[19] B. J. Lipa and D. E. Barrick, "Extraction of sea state from HF radar sea echo: Mathematical theory and modelling," *Radio Sci.*, vol. 21, pp. 81–100, 1986.

[20] L. R. Wyatt, "A relaxation method for integral inversion applied to HF radar measurement of the ocean wave directional spectrum," *Int. J. Remote Sens.*, vol. 11, pp. 1481–1494, 1990.

[21] B. J. Lipa and D. E. Barrick, "Codar wave measurements from a North Sea semisubmersible," *IEEE J. Ocean. Eng.*, vol. 15, no. 2, pp. 119–125, Apr. 1990.
[22] E. W. Gill and J. Walsh, "Extraction of ocean wave parameters from HF backscatter received by a four-element array: Analysis and application," *IEEE J. Ocean. Eng.*, vol. 17, no. 4, pp. 376–386, Oct. 1992.
[23] R. Howell and J. Walsh, "Measurement of ocean wave spectra using narrow beam HF radar," *IEEE J. Ocean. Eng.*, vol. 18, no. 3, pp. 296–305, Jul. 1993.
[24] Y. Hisaki, "Nonlinear inversion of the integral equation to estimate ocean wave spectra from HF radar," *Radio Sci.*, vol. 31, pp. 25–39, 1996.
[25] E. W. Gill, M. L. Khandekar, R. K. Howell, and J. Walsh, "Ocean surface wave measurement using a steerable high-frequency narrow-beam ground wave radar," *J. Atmos. Ocean. Technol.*, vol. 13, pp. 703–713, 1996.
[26] N. Hashimoto and M. Tokuda, "A bayesian approach for estimating directional spectra with HF radar," *Coastal Eng. J.*, vol. 41, pp. 137–149, 1999.
[27] L. R. Wyatt, "Limits to the inversion of HF radar backscatter for ocean wave measurement," *J. Atmos. Ocean. Technol.*, vol. 17, pp. 1651–1666, 2000.
[28] N. Hashimoto, L. R. Wyatt, and S. Kojima, "Verification of a bayesian method for estimating directional spectra from HF radar surface backscatter," *Coastal Eng. J.*, vol. 45, pp. 255–274, 2003.
[29] J. J. Green and L. R. Wyatt, "Row-action inversion of the Barrick-Weber equations," *J. Atmos. Ocean. Technol.*, vol. 23, pp. 501–510, 2006.
[30] L. R. Wyatt, L. J. Ledgard, and C. W. Anderson, "Maximum likelihood estimation of the directional distribution of 0.53 Hz ocean waves," *J. Atmos. Ocean. Technol.*, vol. 14, pp. 591–603, 1997.
[31] L. R. Wyatt, J. Venn, M. D. Moorhead, G. D. Burrows, A. M. Ponsford, and J. van Heteren, "HF radar measurements of ocean wave parameters during NURWEC," *IEEE J. Ocean. Eng.*, vol. OE-11, no. 2, pp. 219–234, Apr. 1986.
[32] L. R. Wyatt and G. J. Holden, "Developments in ocean wave measurement by HF radar," *Inst. Electr. Eng. Proc.-F*, vol. 139, pp. 170–174, 1992.
[33] L. R. Wyatt, S. P. Thompson, and R. R. Burton, "Evaluation of HF radar wave measurement," *Coastal Eng.*, vol. 37, pp. 259–282, 1999.
[34] L. R. Wyatt, J. J. Green, K.-W. Gurgel, J. C. N. Borge, K. Reichert, K. Hessner, H. Günther, W. Rosenthal, O. Saetra, and M. Reistad, "Validation and intercomparisons of wave measurements and models during the EuroROSE experiments," *Coastal Eng.*, vol. 48, pp. 1–28, 2003.
[35] L. R. Wyatt, G. Liakhovetski, H. Graber, and B. Haus, "Factors affecting the accuracy of HF radar wave measurements," *J. Atmos. Ocean. Technol.*, vol. 22, pp. 844–856, 2005.
[36] L. R. Wyatt, "High order nonlinearities in HF radar backscatter from the ocean surface," *Inst. Electr. Eng. Proc.—Radar, Sonar Navigation*, vol. 142, pp. 293–300, 1995.
[37] S. P. Kingsley, A. M. Torregrossa, and L. R. Wyatt, "Analysis of second order HF radar sea spectra recorded in storm conditions," in *Proc. IEEE Oceans'98*, Nice, France, Sep. 1998, pp. 459–462.
[38] D. E. Barrick and B. L. Weber, "On the nonlinear theory for gravity waves on the ocean's surface. Part II: Interpretation and applications," *J. Phys. Oceanogr.*, vol. 7, pp. 11–21, 1977.
[39] B. L. Weber and D. E. Barrick, "On the nonlinear theory for gravity waves on the ocean's surface. Part I: Derivations," *J. Phys. Oceanogr.*, vol. 7, pp. 3–10, 1977.
[40] H. E. Krogstad, J. Wolf, S. P. Thompson, and L. R. Wyatt, "Methods for the intercomparison of wave measurements," *Coastal Eng.*, vol. 37, pp. 235–258, 1999.
[41] L. R. Wyatt and L. A. Binks, "PISCES HF radar and Met Office wave model intercomparisons" U.K. Met Office, Devon, U.K., SCEOS Rep., 2002.
[42] P. E. Dexter and S. Theodorides, "Surface wind speed extraction from HF Skywave radar Doppler spectra," *Radio Sci.*, vol. 17, pp. 643–652, 1982.
[43] L. R. Wyatt and J. J. Green, "HF radar wind measurement" U.K. Met Office, Devon, U.K., SCEOS Rep., 2004.
[44] M. J. Tucker, *Waves in Ocean Engineering: Measurement, Analysis, Interpretation*. Chichester, U.K.: Ellis Horwood, 1991.
[45] B. Candy and S. J. Keogh, "The impact of seawinds scatterometer data on Met Office global analyses and forecasts," Met Office, Exeter, U.K., Forecasting Res. Tech. Rep. 493, Dec. 2006.

Lucy R. Wyatt received the B.Sc. degree in mathematics from the University of Manchester, Manchester, U.K., in 1972, the M.Sc. degree in fluid mechanics from the University of Bristol, Bristol, U.K., in 1973, and the Ph.D. degree in physical oceanography from the University of Southampton, Southampton, U.K., in 1976.

In 1987, she joined the Department of Applied Mathematics, the University of Sheffield, Sheffield, U.K., where she is a Professor. She has been working on the oceanographic applications of HF radar since 1981 when she was a Research Associate with the group led by Ramsay Shearman at the University of Birmingham, Birmingham, U.K. Before, she worked in subsequent research posts in ocean and atmospheric modelling. Her main contribution in the HF radar field has been in the development of inverse methods for measurement of the directional wave spectrum. She has founded a small company, Seaview Sensing Ltd., Sheffield, U.K., to make the software developed at University of Sheffield more widely available.

J. Jim Green, photograph and biography not available at the time of publication.

Andrew Middleditch received the Ph.D. degree in applied mathematics from the University of Sheffield, Sheffield, U.K., in 2006. His thesis concerned the study of spectral analysis techniques in HF radar oceanography.

He currently works for Seaview Sensing Ltd., Sheffield, U.K.

Mike D. Moorhead received the B.Sc. degree in electronic and electrical engineering from the University of Manchester, Manchester, U.K., in 1968 and the Diploma in business management from the Polytechnic of Central London, london, U.K., in 1978.

He is the Managing Director of Neptune Radar Limited, Sandhurst, U.K., which he founded in 1983 to provide solutions to HF radar design, operation, or analysis requirements. The company has moved from a specialized consultancy to services for HF-radar-based metocean data measurement and ship surveillance. His vision for the future of HF radar is reflected in the design and development of the Pisces radar. Now that it is in operational use, his focus is on driving down ownership costs and increasing data availability. Previously, he served in the Royal Air Force as an Engineering Officer where he worked on HF communications systems, radar, and embedded system software. He was then appointed Research Fellow at the University of Birmingham, Department of Electronic and Electrical Engineering working on HF radar technology for both sky wave and surface wave applications.

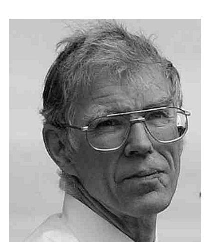

John Howarth has studied the dynamics of tidally dominated continental shelf seas, including their response to meteorological and density forcing, since 1969, when he joined what was called then the Institute of Coastal Oceanography and Tides and is now called the Proudman Oceanographic Institute, Liverpool, U.K., both U.K. Natural Environment Research Council institutes. The studies have been on all scales from turbulence upwards and have concentrated on obtaining, analyzing and interpreting measurements and their synthesis with theory and numerical models.

Martin Holt graduated from Oxford University in 1983 with first class honors in mathematics. He received the M.Sc. degree in numerical solution of differential equations from Reading University, Reading, U.K. and the Ph.D. degree modeling frontal rainbands and conditional symmetric instability from Reading University's Department of Meteorology, in 1990.

He joined the Met Office, Exeter, U.K., in 1984, and in 1990, he became responsible for development of the operational wave forecast models run there. Since 1996, he has been the Manager of the team developing the operational wave models and shelf seas models.

Simon Keogh received the Ph.D. degree in the remote sensing of sea surface temperature from the University of Southampton, Southampton, U.K., in 1998.

In 1999, he joined the U.K. Met Office, Exeter, U.K., where he is currently a Research Scientist working on the assimilation of scatterometer ocean surface wind vectors into numerical weather prediction models.